Superposition and Polarization Effects on the Electron Density of Lone Pairs *

Ivar Olovsson, Halina Ptasiewicz-Bak **, and Garry J. McIntyre ***
Institute of Chemistry, University of Uppsala, S-751 21 Uppsala, Sweden

Z. Naturforsch. **48a**, 3–11 (1993); received January 30, 1992

There appears to be conflicting experimental evidence on the redistribution of the electron density in the lone-pair and other regions of a molecule due to the interaction with its nearest neighbours. In some experimental as well as theoretical deformation density maps a decrease in the lone-pair density has been reported, whereas in other cases an increase has been found. It appears that two major, counteracting factors are responsible for these differences (apart from experimental errors in the diffraction studies and limited accuracy in the theoretical calculations): an increase in the lone-pair density is expected due to the polarizing influence of the neighbours, whereas simple superposition of the isolated monomer deformation densities will lead to an apparent decrease due to the overlap with the negative contours of the neighbouring atom. Depending on which of these factors is the dominant one, an increase or decrease may thus be observed.

These points are illustrated by recent results on nickel sulfate hexahydrate and some other hydrogen-bonded compounds. The electron density based on the fitted deformation functions of all atoms in the structure is compared with the individual densities calculated from deformation functions of the separate monomers. In this way the effects of simple superposition of the individual densities have been studied, and a partitioning of the electrostatic and polarization contributions to the hydrogen bonds and other relatively weak bonds to the oxygen lone-pairs attempted.

Key words: Electron density; Superposition effects; Polarization effects; Lone pairs; Hydrogen bonds.

Introduction

For assemblies of small molecules containing only light elements qualitative agreement between the electron density determined in diffraction experiments and that from theoretical calculations is attainable. In order to obtain quantitative agreement, however, there still remain several difficulties to be overcome. For hydrogen-bonded structures this applies in particular to the electron density in the lone-pair regions. As an example we may take the extensively studied oxalic acid dihydrate. In Fig. 1 are shown some experimental and theoretical determinations of the deformation density, $\Delta\varrho = \varrho(\text{total}) - \sum_i \varrho_i(\text{spherical atoms})$. There are quite noticeable differences amongst the experimental and theoretical densities. In one of the theoretical studies (Breitenstein et al. [1]) there was even predicted a *decreased* density in the lone-pair region around O3 which accepts a hydrogen-bond from the O–H group of the oxalic acid molecule, whereas Krijn and Feil [2] predicted an *increased* density in this region, in agreement with both experimental results. This disagreement is clearly due to differences in the details of the theoretical calculations (size of the basis sets, basis set superposition effects, etc.). The experimental maps agree reasonably well, but being conventional difference maps, based on $F_o - F_c$, they represent necessarily superpositions of the deformations of the individual atoms.

In the case of compounds containing heavier elements, like transition metals, the experimental as well as theoretical difficulties are much more severe. Besides the ordinary experimental problems with absorption, extinction etc., the scattering due to the valence electrons is only a very small proportion of the total scattering. Relatively speaking, however, the situation for the later members of the first transition metal series (e.g. Co, Ni) is more favorable than for the earlier members as the successive contraction of the 3d electrons towards the nucleus results in a higher

* Presented at the Sagamore X Conference on Charge, Spin, and Momentum Densities, Konstanz, Fed. Rep. of Germany, September 1–7, 1991.

** Permanent address: Institute of Nuclear Chemistry and Technology, Dorodna 16, 03-195 Warsaw, Poland.
*** The Studsvik Neutron Research Laboratory, University of Uppsala, S-611 82 Nyköping, Sweden.
Present address: Institut Laue-Langevin, 156X, F-38042 Grenoble Cedex, France.
Reprint requests to Prof. I. Olovsson, Institute of Chemistry, University of Uppsala, Box 531, S-751 21 Uppsala, Sweden.

0932-0784 / 93 / 0100-0003 $ 01.30/0. – Please order a reprint rather than making your own copy.

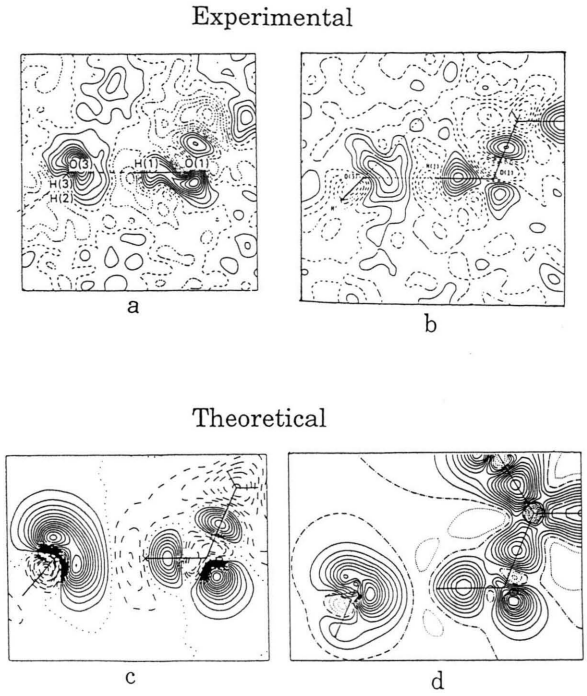

Fig. 1. $H_2C_2O_4 \cdot 2\,H_2O$. Experimental (X–N) and theoretical deformation densities: (a) Stevens and Coppens [15]; (b) Dam, Harkema and Feil [16]; (c) Breitenstein et al. [1]; (d) Krijn and Feil [2]. Contour levels in this and the following figures, unless stated otherwise: ± 0.05 eÅ^{-3}.

proportion of scattering due to these electrons at high Bragg angles. In spite of this, the experimental deformation densities of transition-metal complexes found in the current literature mostly show a lot of spurious peaks which cannot easily be interpreted in terms of true bonding effects.

An experimental study of the electron density in the ordinary tetragonal form of $NiSO_4 \cdot 6\,D_2O$ has earlier been made by the present authors [3]. More recently, the investigation has been repeated at 25 K on $NiSO_4 \cdot 6\,H_2O$ [4]. The object was in the first place to determine the electron density around the nickel ion, but it was also interesting to study whether it would be possible to obtain reasonable densities of the water molecules in the presence of such a heavy scatterer as nickel. The present paper will concentrate on the deformation density of the water molecules and discuss a simple technique to remove the effects of superposition in the lone-pair region. A comparison is then made with the results from accurate experimental and theoretical electron density studies of some other hydrogen-bonded compounds.

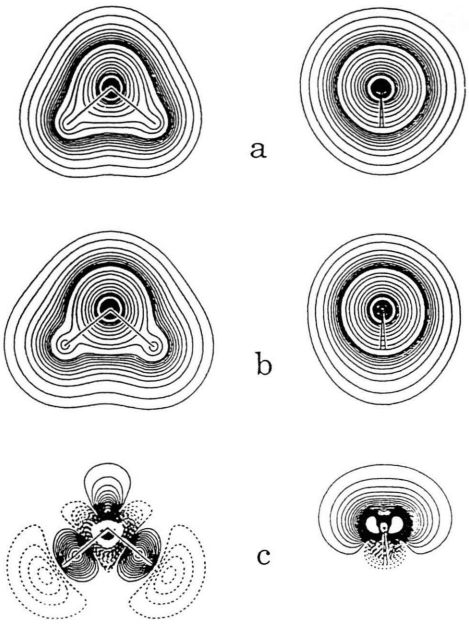

Fig. 2. Theoretical electron density maps for a free H_2O molecule; left: in the molecular plane, right: bisecting the H–O–H angle. (a) $\varrho(H_2O)$; (b) $\sum \varrho_i$(atoms); (c) difference (a)–(b) (from Hermansson [5]).

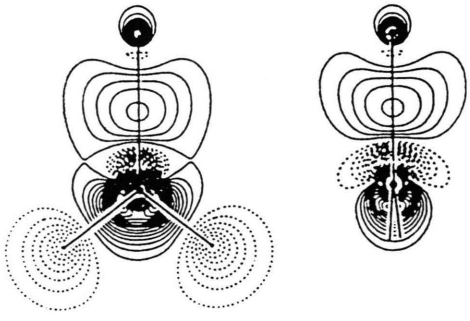

Fig. 3. $Be^{2+} \cdot H_2O$ model complex. Theoretical deformation density $\varrho(Be^{2+} \cdot H_2O) - [\varrho(Be^{2+}) + \varrho(H_2O)]$ (from Hermansson, Olovsson and Lunell [6]).

Theoretical Calculations of the Electron Density of the Isolated Water Molecule and the Influence of Cations and Hydrogen Bonds

The total electron density of the isolated water molecule from ab initio calculations by Hermansson [5] is shown in Figure 2a. The corresponding density obtained on superimposing the spherical density of the free oxygen and hydrogen atoms (the "promolecule" density) is shown in Figure 2b. The close resemblance

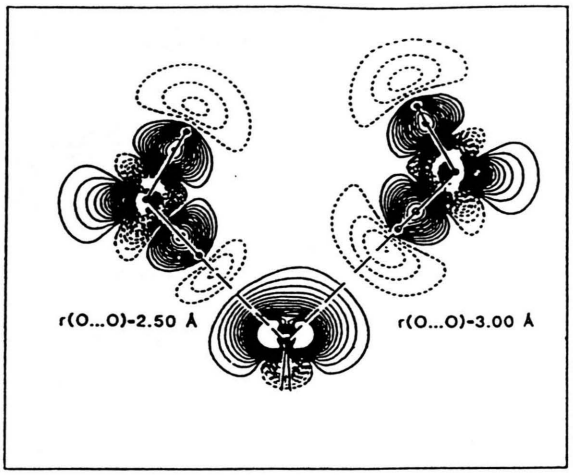

a

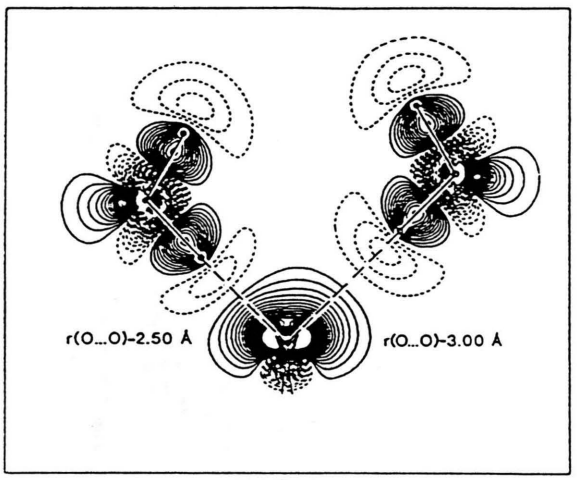

b

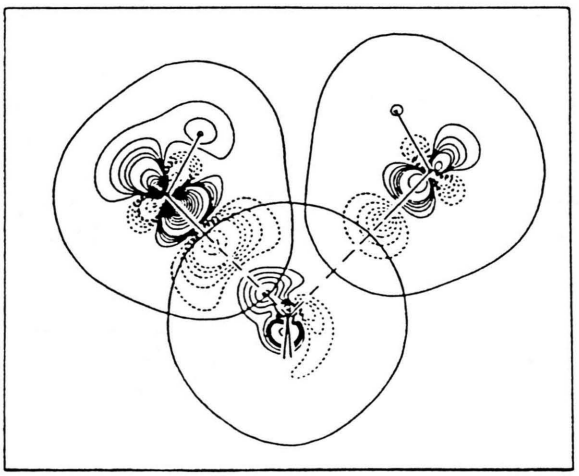

c

Fig. 4. Trimer of water. Theoretical deformation density maps in a model complex. (a) ϱ(trimer) $-\sum \varrho_i$(atoms); (b) $\sum \varrho_i$(free H_2O) $-\sum \varrho_i$(atoms); (c) difference (a)–(b). Contour levels in (a) and (b): ± 0.05 eÅ^{-3}, in (c) ± 0.01 eÅ^{-3} (from Hermansson [5]).

between these two maps illustrates that even formation of strong covalent bonds between the atoms has only a quite small effect on the total density. In particular, a concentration of the electron density in the lone-pair directions is not noticeable at all in the total density. The difference between Fig. 2a and 2b (the deformation density, $\Delta\varrho$, relative to spherical atoms) is

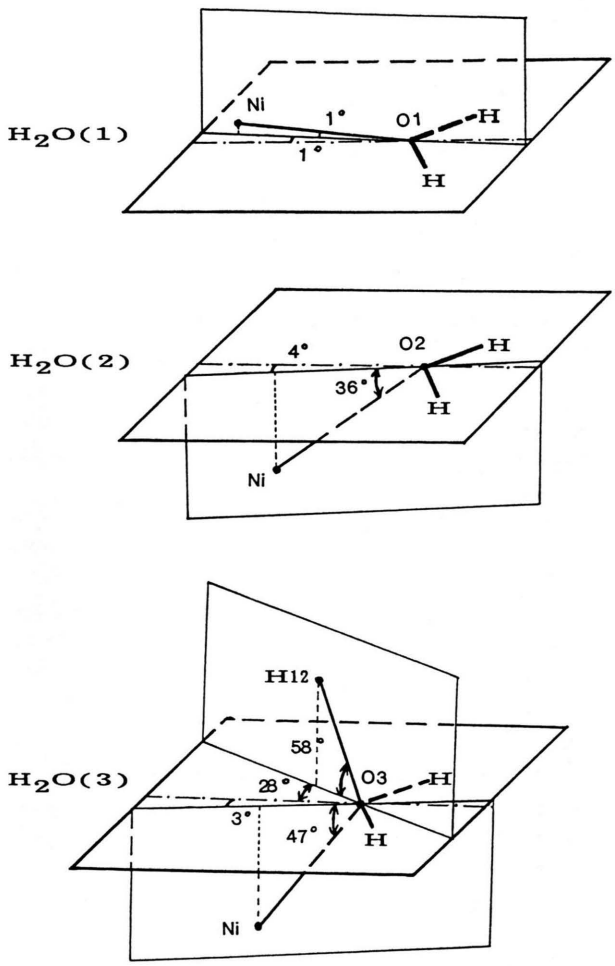

Fig. 5. $NiSO_4 \cdot 6\,H_2O$. Coordination of the three independent water molecules: $H_2O(1)$ is bonded to Ni in the plane of the water molecule; $H_2O(2)$ is bonded to Ni along a tetrahedral direction, but lacks a second neighbour in the other tetrahedral direction; $H_2O(3)$ is tetrahedrally bonded to Ni and $H_2O(1)$.

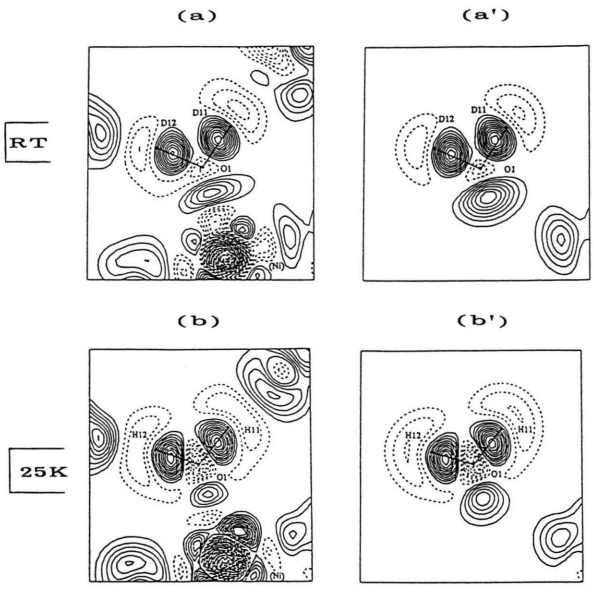

Fig. 6. $NiSO_4 \cdot 6\,H_2O$. Experimental, modelled deformation density (static) in the plane of $H_2O(1)$ at room temperature (RT) and 25 K. In figures (a) and (b) all deformation functions are included; in figures (a′) and (b′) only the deformation functions centred on the water molecule are included (from McIntyre, Ptasiewicz-Bak and Olovsson [3], and Ptasiewicz-Bak, McIntyre and Olovsson [4]).

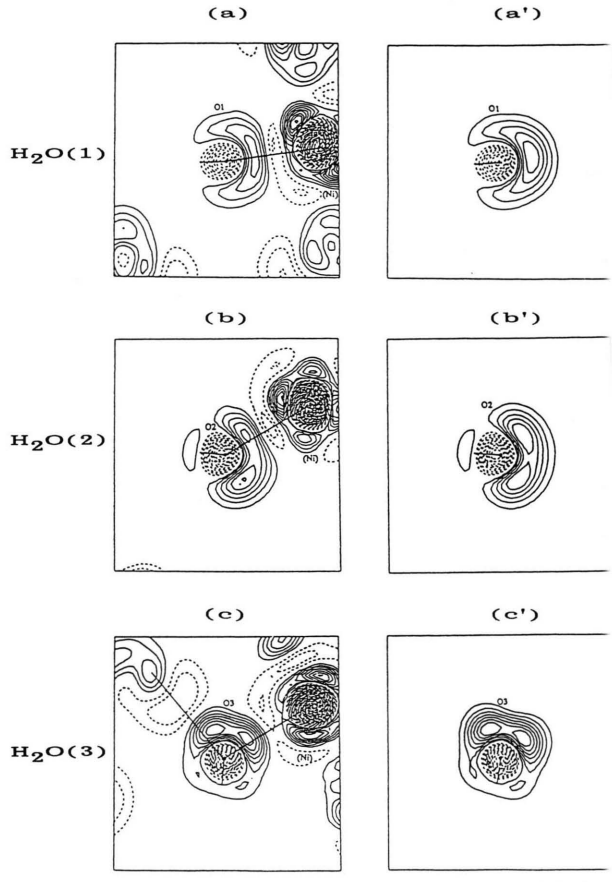

Fig. 7. $NiSO_4 \cdot 6\,H_2O$ at 25 K. Experimental, modelled deformation density (static) in planes perpendicular to the water planes and bisecting the H–O–H angles; see further Figure 6.

shown in Fig. 2c. For the later discussion it should be noticed that even the deformation density extends smoothly over the whole non-bonded region around oxygen with no extension of the outer contours in the direction of the individual lone-pair lobes.

The influence of cations on the electron density of water has been studied in model calculations of some $Me^{n+} \cdot H_2O$ complexes ($Me^{n+} = Li^+$, Mg^{2+}, Be^{2+} and Al^{3+}). The deformation maps for $Be^{2+} \cdot H_2O$ are shown in Figure 3. The lone-pair density of the water oxygen atom is clearly concentrated in the direction towards Be^{2+}. There is an analogous effect when a hydrogen bond is accepted by water in the lone-pair direction. This is illustrated by the $O \cdots O$ bond of 2.50 Å in Figure 4c. In both cases we neglect the decrease close to the oxygen nucleus, a region where neither the theoretical nor the experimental densities are reliable.

Deformation Density of the Water Molecules in $NiSO_4 \cdot 6\,H_2O$

This complex is particularly interesting in this context as it contains three independent water molecules which are coordinated quite differently to nickel as shown in Figure 5. It is possible to detect experimentally the subtle effects due to this difference in coordination? The experimental details of these studies are published in [3] and [4]. The results illustrated here are derived from multipole refinements of the X-ray data using atom-centered deformation functions related to spherical harmonics [7]. The maps shown give the electron density corresponding to the sum of these deformation functions and thus represent a "modelled" deformation density relative to spherical atoms. This type of deformation density has the advantage that experimental noise present in ordinary difference ($F_o - F_c$) maps, as presented in Fig. 1, has to a large extent been filtered out. All maps shown here are static; the corresponding dynamic maps are practically identical.

The model deformation densities in the plane of $H_2O(1)$ at RT and 25 K are shown in Figs. 6a and b; the corresponding maps of $H_2O(2)$ and $H_2O(3)$ are very similar. The densities in the "lone pair planes" perpendicular to the planes of $H_2O(1)$, $H_2O(2)$ and $H_2O(3)$ at 25 K are shown in Figs. 7a, b and c. Qualitatively the deformation densities agree with the theoretical results for free water (Fig. 2c), but there are clear differences, particularly in the non-bonded regions around oxygen. In an attempt to eliminate effects of simple superposition of neighbouring atoms, partial model deformation densities have also been calculated, Figs. 6a′ and b′ and Figs. 7a′, b′, c′. Here only the deformation density functions centered on the respective water molecules have been plotted. There is now a much closer agreement with the free molecule density. However, we notice a certain concentration in the direction towards the coordinating Ni^{2+} ion for $H_2O(1)$ and $H_2O(2)$ and in the two tetrahedral directions for $H_2O(3)$, which accepts Ni^{2+} and a hydrogen bond from $H_2O(1)$. If we compare with the results of the theoretical calculations of the previous section it appears possible that the concentration observed in the experimental maps in the directions towards Ni^{2+} (Figs. 7a′ and 7c′) and towards an approaching hydrogen-bond donor (Fig. 7c′) is caused by these interactions. The maps at RT, corresponding to Fig. 7, are surprisingly similar (see [3]).

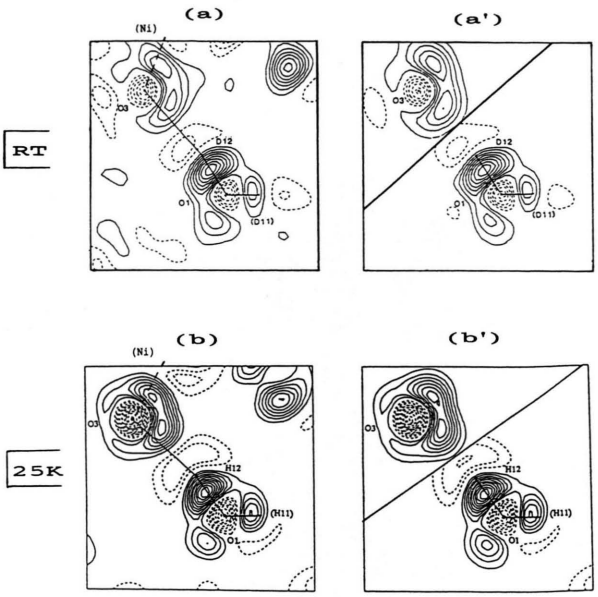

Fig. 8. $NiSO_4 \cdot 6\,H_2O$. Experimental, modelled deformation density in the hydrogen bond between water $H_2O(1)$ and $H_2O(3)$. (a) and (b) All deformation functions included. (a′) and (b′) Only deformation functions centred on $H_2O(3)$ (upper left) or on $H_2O(1)$ (lower right) included (from [3] and [4]).

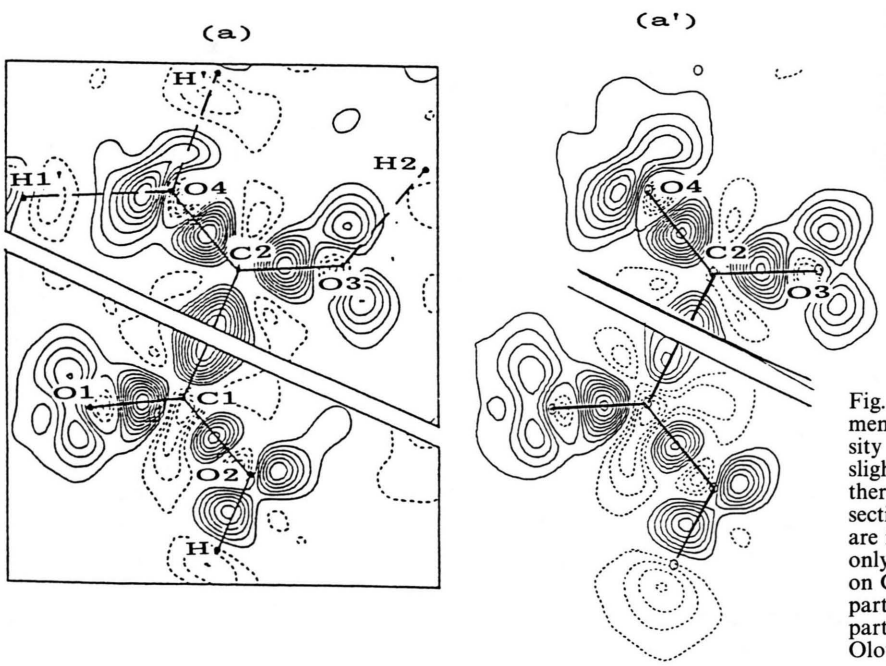

Fig. 9. $NaHC_2O_4 \cdot H_2O$. (a) Experimental, modelled deformation density of the $HC_2O_4^-$ ion (the ion is slightly twisted, and the density is therefore calculated in two different sections). All deformation functions are included. (a′) as in (a), but with only deformation functions centred on C2, O3 and O4 included (upper part) or on C1, O1 and O2 included (lower part) (from Delaplane, Tellgren, and Olovsson [8], [10]).

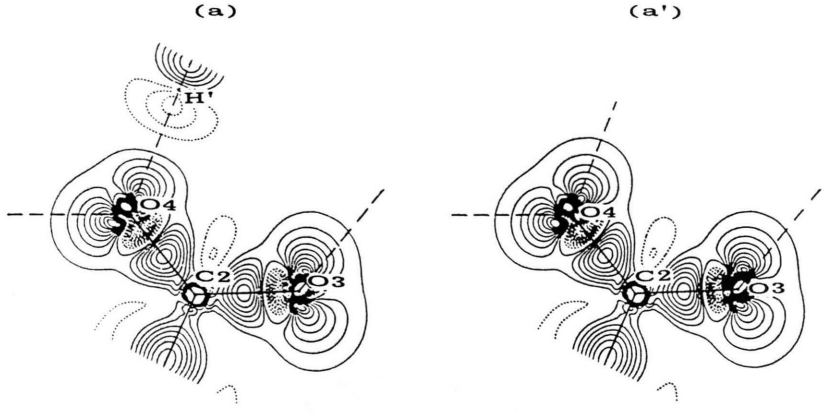

Fig. 10. Theoretical deformation density of $HC_2O_4^-$ (cf. Figure 9). (a) Superposition of two isolated ions in the same relative positions as in crystalline $NaHC_2O_4 \cdot H_2O$; (a') Isolated ion (from Lunell [9]).

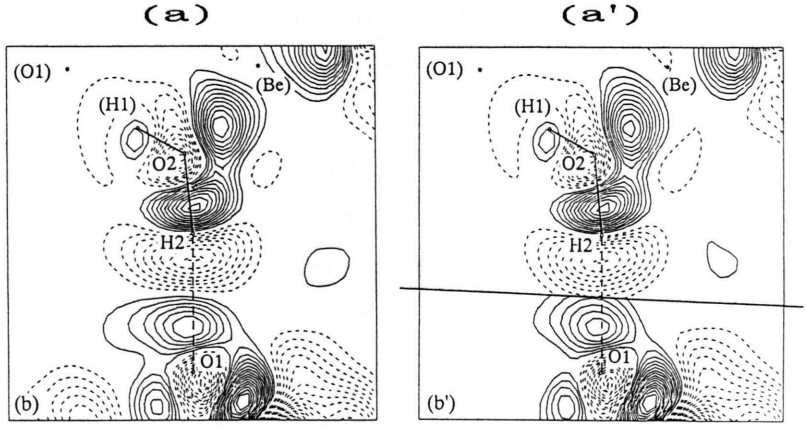

Fig. 11. $BeSO_4 \cdot 4\,H_2O$. Experimental, modelled deformation density in the hydrogen bond between water $H_2O(2)$ and sulfate oxygen O1. Contour levels ± 0.025 eÅ^{-3}. (a) All deformation functions included. (a') Only deformation functions centered on $H_2O(2)$ (upper part) or on SO_4^{2-} (lower part) included (from Kellersohn, Delaplane and Olovsson [11]).

Superposition Effects

Hydrogen-bonded Systems

The model deformation density maps for $NiSO_4 \cdot 6\,H_2O$ illustrate that addition of the deformation density functions of the surrounding atoms can cause a clear distortion of the water density, in particular a decrease of the density in the non-bonded region of oxygen. This simple superposition effect is clearly illustrated by theoretical calculations on the water trimer shown in Fig. 4a. The water density in the direction of the short hydrogen bond (2.50 Å) is considerably reduced as compared to the other direction (3.00 Å); we may consider the density in the latter direction as essentially undistorted. However, simply adding the deformation densities of the free monomers gives an almost identical map, Figure 4b. It thus appears that the reduced density in Fig. 4a is essentially due to a superposition of the negative region of the donating O–H group onto the positive region of the accepting oxygen atom. The true distortion due to hydrogen bonding is given by the difference between Figs. 4a and 4b, as shown in Fig. 4c (note that the contour levels are more detailed here). We notice qualitatively the same features in this map as in the original monomers (Fig. 4b), i.e. the electron density features which already exist in the free monomers are further strengthened by the hydrogen-bond interaction. In other words, the original polarity of the isolated molecules is further increased as a hydrogen bond is formed.

In $NiSO_4 \cdot 6\,H_2O$ there is a hydrogen bond between the water molecules $H_2O(1)$ and $H_2O(3)$. The model deformation density in this bond at RT and 25 K is shown in Figures 8a, b. The partial densities based on each water molecule separately are shown in Figures 8a', b'. We notice again that the superposition of the separate densities results in a considerable modification of the lobe on O3 in the direction of the hydrogen bond.

The distortion due to superposition is also observed in $NaHC_2O_4 \cdot H_2O$. In the crystal structure, the $HC_2O_4^-$ ions are coupled into linear chains by relatively strong hydrogen bonds, O(4) ··· O(2′) distance = 2.57 Å (Fig. 9); there are also much weaker hydrogen bonds of 2.79 Å transverse to these chains. In the experimental deformation density the "lone-pair lobe" of oxygen O4, which accepts the strong hydrogen bond, is considerably reduced in comparison with the other lobe, Figure 9a. This may seem strange, as one would expect that the electrons would be shifted more strongly towards the proton donor in the shorter hydrogen bond. Theoretical calculations [9] demonstrate clearly that the apparent decreased density in the chain direction is simply a superposition effect: The theoretical deformation density of an isolated $HC_2O_4^-$ ion is shown in Figure 10a′. The two lone-pair lobes of O4 are very nearly identical. When the densities of two such isolated ions are juxtaposed (Fig. 10a), the negative contours around the proton donor (H′) will cause an apparent compression of the contours of the lone-pair lobe of O4 in the chain direction. In order to eliminate this superposition effect in the experimental density, a partial model deformation density map based on only the deformation functions centered on C2, O3 and O4 has also been plotted, Fig. 9a′. We notice that the lobes around O4 are now more equal, although the effect is still not quite eliminated.

Another example of the superposition effect in hydrogen bonds is illustrated by $BeSO_4 \cdot 4\,H_2O$, Figure 11. The model deformation density in the hydrogen bond donated by $H_2O(2)$ to sulfate oxygen O(1) is shown in Fig. 11a. The partial density based on only the water and sulfate deformation functions, respectively, is shown in Figure 11a′. The effect is very similar to the previous cases discussed above.

Nickel(II) Ion

The Ni^{2+} ion in $NiSO_4 \cdot 6\,H_2O$ is octahedrally coordinated by six water molecules. The deformation density in Figs. 12a, b shows the features expected for a $d_\varepsilon^6 d_\gamma^2$ electron configuration, with the diagonally directed d_ε orbitals (d_{xy}, d_{xz} and d_{yz}) all filled but with only one electron in each of the two d_γ orbitals (d_{z^2} and $d_{x^2-y^2}$): a deficiency in the directions towards the water ligands as compared to the diagonal directions (see further [3]). The deformation maps of nickel with the adjacent water deformation functions omitted give a much clearer picture of the nickel electron density,

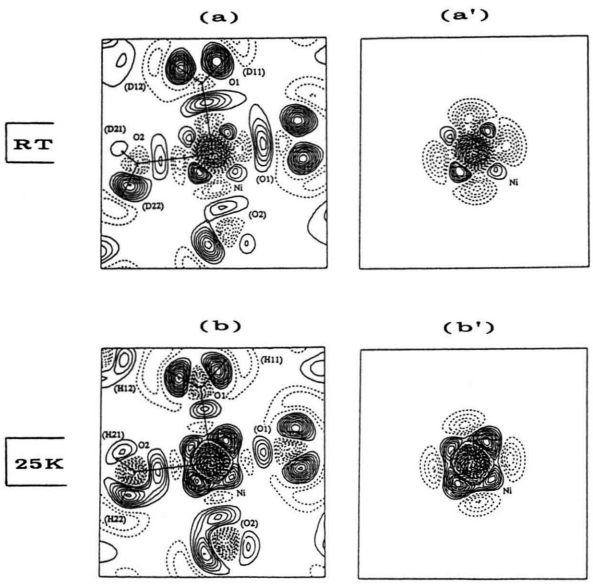

Fig. 12. $NiSO_4 \cdot 6\,H_2O$. Experimental, modelled deformation density around Ni, calculated in the plane through Ni, O(1) and O(2). All deformation functions included in (a) and (b), only the Ni functions in (a′) and (b′).

Figures 12a′, b′. The superposition with the positive "lone-pair peaks" of water have resulted in considerably reduced negative peaks around nickel in Figs. 12a, b as compared to Figs. 12a′, b′, whereas the positive peaks in the diagonal directions are practically not affected at all.

In the next section we will interpret the superposition effect in terms of our common concepts used in discussing hydrogen bonds and other weak interactions.

Partitioning of Intermolecular Interactions

When discussing various aspects of hydrogen bonding it has often been found useful to partition the total interaction energy in the following components: Electrostatic (Coulomb), polarization, charge transfer, exchange and dispersion energy (cf. [12]). The electrostatic contribution corresponds to the energy change that would result if the free constituent molecules, A and B, were somehow brought together into the relative positions in which they appear in the hydrogen-bonded complex, without deforming the original monomer charge distributions and without any electron exchange taking place. The polarization contri-

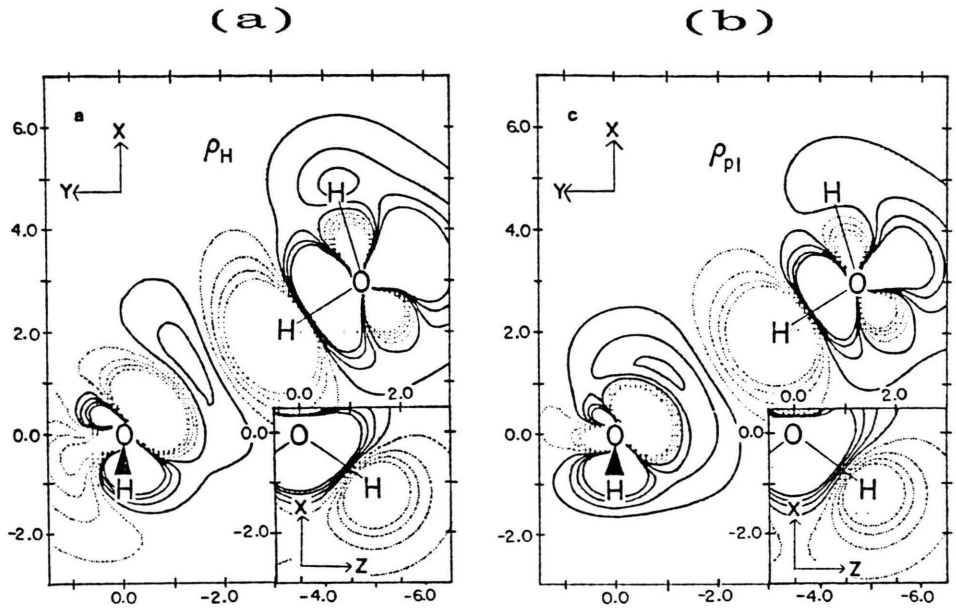

Fig. 13. Water dimer. Theoretical deformation density relative to the isolated monomers. (a) The total deformation due to hydrogen bonding; (b) the polarization component (from Yamabe and Morokuma [14]).

bution corresponds to the additional energy gain on deforming the monomer charge distributions from the previous hypothetical situation to a state more closely resembling the final hydrogen-bond situation, but still without any transfer of electrons between the original constituents. For a discussion of the limitations of the partitioning scheme cf. [13].

It is then clear that the superposition of the electron distributions of the free monomers discussed in the previous section precisely corresponds to the model used to calculate the (classical) electrostatic part of the energy of the hydrogen-bond interaction between the two systems. The difference between the electron distributions of the hydrogen-bonded complex and the original monomers, $\varrho(\text{complex}) - \sum_i \varrho_i(\text{monomers})$, corresponds to the total electron redistribution due to the remaining components of the hydrogen-bond interaction. This difference is shown for the water dimer in Figure 13 a. Yamabe and Morokuma [14] also made an analysis of the redistribution of the electron density associated with each of the components separately; the polarization part is shown in Figure 13 b. One notices that Figs. 13 a and 13 b are qualitatively very similar. This result and the relative magnitudes of the partial energies involved suggest that the major part of the electron redistribution due to hydrogen bonding may be interpreted as a polarization effect. This appears to be true for weak and moderately strong hydrogen bonds.

Returning to the maps of the water trimer, the superposition map in Fig. 4 b thus represents the electrostatic model of the system, whereas the redistribution illustrated in Fig. 4 c may be interpreted as mainly a polarization effect.

The experimental deformation maps $\Delta\varrho = \varrho(\text{total}) - \sum_i \varrho_i(\text{atoms})$ clearly include the superposition effect (as well as the redistribution on forming molecules from the constituent atoms). This effect should have been eliminated in the partial deformation maps earlier shown for $NiSO_4 \cdot 6\,H_2O$, $NaHC_2O_4 \cdot H_2O$ and $BeSO_4 \cdot 4\,H_2O$. However, these maps still show distortion of the monomer densities. From comparison with the analysis of Yamabe and Morokuma [14] we may suggest that these distortions are mainly polarization effects due to interaction with the neighbours. Accordingly, it appears that when superposition effects are removed, polarization is expected to lead to an increase in the lone-pair density.

The above partitioning scheme has been primarily applied to hydrogen bonding, but it may also be useful when discussing other types of weak interactions, e.g. in metal complexes with weak ligand fields like in

$NiSO_4 \cdot 6\ H_2O$. The distortions of the lone-pair distributions noticed earlier in Figs. 7a′–c′ would then be interpreted mainly as polarization effects.

Conclusions

Partial model deformation maps may give qualitative information about distortions due to the interaction with the neighbours both for hydrogen-bonded complexes and metal complexes with weak ligand fields. Superposition of the isolated monomer densities corresponds to an "electrostatic" model of the density of the complex: the lone-pair deformation density of the acceptor molecule then *appears* to *decrease* when a hydrogen bond is formed; the intrinsic lone-pair density is of course not affected as no deformation is allowed in the electrostatic model. The polarization component separately will lead to an *increase* in the lone-pair density. The electrostatic and polarization contributions dominate the total interaction for weak and moderately strong hydrogen bonds. Depending on the relative influence on the density of these two components the resulting lone-pair density on the acceptor molecule may then either decrease or increase as a hydrogen bond is formed. In $NiSO_4 \cdot 6\ H_2O$, $NaHC_2O_4 \cdot H_2O$ and $BeSO_4 \cdot 4\ H_2O$ the bonding lone-pair densities decrease since the electrostatic contribution dominates. Oxalic acid dihydrate offers an example where the effect due to polarization appears to dominate (Figure 1).

The above partial model deformation density maps naturally represent just one way of partitioning the density between the various constituents (molecules/ions) in the crystal (derived by a least-squares fitting procedure of chosen deformation functions to the observed electron density). Further cases must be examined to test whether these types of partial maps are reproducible and are physically reasonable.

[1] M. Breitenstein, H. Dannöhl, H. Meyer, A. Schweig, R. Seeger, U. Seeger, and W. Zittlau, Int. Rev. Phys. Chem. **3,** 335 (1983).
[2] M. P. C. M. Krijn and D. Feil, J. Chem. Phys. **89,** 4199 (1988).
[3] G. J. McIntyre, H. Ptasiewicz-Bak, and I. Olovsson, Acta Cryst. **B 46,** 27 (1990).
[4] H. Ptasiewicz-Bak, G. J. McIntyre, and I. Olovsson, submitted to Acta Cryst. B (1992).
[5] K. Hermansson, Acta Univ. Upsaliensis No. 744, 1984.
[6] K. Hermansson, I. Olovsson, and S. Lunell, Theoret. Chimica Acta (Berl.) **64,** 265 (1984).
[7] F. Hirschfeld, Isr. J. Chem. **16,** 226 (1977).
[8] R. G. Delaplane, R. Tellgren, and I. Olovsson, Acta Cryst. **B 46,** 361 (1990).
[9] S. Lunell, J. Chem. Phys. **80,** 6185 (1984).
[10] R. G. Delaplane, R. Tellgren, and I. Olovsson, in preparation (1992).
[11] T. Kellersohn, R. G. Delaplane, and I. Olovsson, in preparation (1992).
[12] K. Morokuma, J. Chem. Phys. **55,** 1236 (1971).
[13] I. Olovsson, in: Electron and Magnetization Densities in Molecules and Crystals (P. Becker, ed.), Plenum, New York 1980, pp. 883–890.
[14] S. Yamabe and K. Morokuma, J. Amer. Chem. Soc. **97,** 4458 (1975).
[15] E. D. Stevens and P. Coppens, Acta Cryst. **B 36,** 1864 (1980).
[16] J. Dam, S. Harkema, and D. Feil, Acta Cryst. **B 39,** 760 (1983).